CO12-1

Instrumental neutron activation analysis of Ir in PtIr alloy

T. Miura[1], R. Okumura[2], Y. Iinuma[2] and H. Yoshinaga[2]

[1]*Advanced Industrial Science and Technology (AIST), National Metrology Institute of Japan*
[4]*Institute for Integrated Radiation and Nuclear Science, Kyoto University*

INTRODUCTION: Neutron activation analysis using comparator standard is recognized as a potential primary ratio method [1]. Despite the potential of neutron activation analysis as primary ratio method, the evaluation the measurement capability and the measurement uncertainty are required in any analysis. In general, there are three main components of uncertainty in neutron activation analysis, that is, sample preparation uncertainty, neutron flux homogeneity, and gamma ray measurement uncertainty. Usually, flux monitor is used to correct the neutron flux heterogeneity. However, although the flux monitor can correct the neutron flux variation using the count rate of the known amount of the monitor nuclide, it does not reflect the neutron flux of the actual sample. The most practical method to eliminate neutron flux heterogeneity to improve gamma ray measurement uncertainty is an internal standard method [2, 3]. In this study, we presented that capability of instrumental neutron activation analysis for determination of Ir in the PtIr alloy. Pt-Ir alloys are known to be stable and very difficult to completely decompose.

EXPERIMENTS: The PtIr (foil, 0.025 mm thick, 25 mm×25 mm, Alfa Aesar, 99.9 %, Lot No. I24T008) purchased from FUJIFILM Wako Pure Chemical Corporation. The composition ratio of the PtIr foil was indicated by the manufacture as Pt:Ir; 90:10. High purity Ir metal (Alfa Aesar, powder, 99.99 %, Lot No. M17E046) was used for calibration standard for Ir. The Au solution prepared from high purity metal was added in the irradiation samples for internal standard. The neutron irradiations for Ir in the PtIr alloy sample performed by KUR TcPn (thermal neutron flux: 8×10^{10} $cm^{-2}s^{-1}$) for 20 min. The irradiated samples were cooled appropriately. The gamma rays form irradiated samples were measured using ORTEC GEM 25185 Ge detector with Laboratory Equipment Corporation MCA 600. The measure radioactive isotopes were ^{192}Ir, ^{194}Ir and ^{198}Au.

RESULTS: Analytical results of Ir in the PtIr alloy were shown in Table 1. The measured values were in good agreement with manufacture indicated value. Analytical results demonstrate the effectiveness of instrumental neutron activation analysis.

Table 1. Analytical results of Ir in the PtIr alloy

Sample No.	Measured values, Ir g/g
1	0.0993±0.002
2	0.0992±0.004

REFERENCES:

[1] R. Greenberg *et al.*, Spectrochim. Acta B, **66** (2011) 193-241.
[2] T. Miura *et al*., Talanta, **82** (2010) 1143-1148.
[3] T. Miura *et al.*, J. Radioanal. Nucl. Chem., **303** (2015) 1417-1420.
[4] NuDat 2, National Nuclear Data Center in Brookhaven National Laboratory, https://www.nndc.bnl.gov/nudat2/index.jsp

Fundamental Study of Superposition of Coherent Transition Radiation Using a Ring-type Resonator

N. Sei and T. Takahashi[1]

Research Institute for Measurement and Analytical Instrumentation, National Institute of Advanced Industrial Science and Technology
[1]Institute for Integrated Radiation and Nuclear Science, Kyoto University

INTRODUCTION: Terahertz light sources based on linear accelerators are characterized by a high repetition frequency. In order to utilize this feature to develop a high-peak-power terahertz light, we have studied to confine coherent transition radiation (CTR) in an optical resonator to achieve pulse superposition, and to extract it from the resonator using Fresnel reflection [1]. By us-ing Tsurupika, which has low absorption in the terahertz region, as an output coupler, we success-fully observed that CTR pulses are superimposed in the optical resonator.

EXPERIMENTS: An electron beam with energy of 39 MeV was used for the pulse superposition experiments at the L-band linear accelerator of Kyoto University (KURNS-LINAC). The repetition and duration of the electron-beam macropulse were 15 Hz and 100 ns, respectively. The electron beam with a current of 1.0 μA passed through an aluminum collimator generated CTR by penetrat-ing two aluminum-deposited polyethylene films that composed a ring-type optical resonator. The generated CTR orbited the ring-type resonator with a circumference of 923 mm which correspond-ed to four times the CTR pulse interval. Therefore, the CTR pulses circulating around the resonator were superimposed on the CTR pulses generated after one rotation. A Tsurupica substrate with a thickness of 2 mm was inserted at 45° to the CTR beam in the part of the resonator that formed a parallel CTR beam. A portion of the superimposed CTR pulse was extracted from the resonator by Fresnel reflection on this substrate, and temporal structure and spectrum of the CTR pulses were measured in an experimental room.

RESULTS: Figure 1 shows CTR power measured by a Si bolometer while adjusting the circum-ference of the resonator. The CTR power in the figure is normalized to the power of a non-superimposed CTR pulse measured by inserting a millimeter-wave absorber into the resonator. The CTR power almost perfect synchronization condition of the resonator was nearly twice as high as that without superimposition. Moreover, the CTR power had minimums when a detuning length of the resonator was ±1 mm. Because the CTR spectrum had a maximum around a wavenumber of 5 cm^{-1}, it was suggested that the second-lap CTR pulses superimposed with the first-lap CTR pulses, resulting in a decrease in CTR power. Therefore, it was confirmed that the electric field of the CTR pulses was superimposed by the resonator. At higher wavenumbers, the superposition of the CTR pulses becomes more effective because a diffraction loss in the resonator can be reduced. Our experimental results demonstrate that CTR pulses with high peak power can be generated by the pulse superposition.

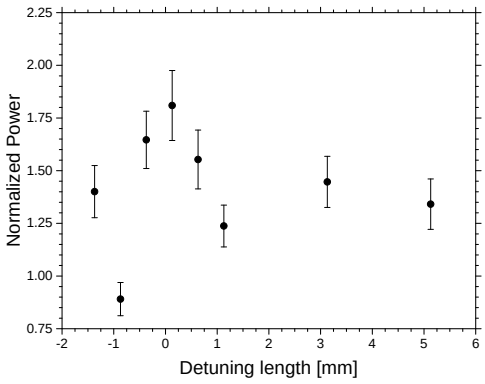

Fig. 1. CTR power vs. detuning length

REFERENCES:

[1] N. Sei and T. Takahashi, submitted to Appl. Opt.

CO12-3

SEM-EDS analysis of enlarged particles prepared by spraying $(U,Zr)O_2$ particle -immersed solution for decommissioning of Fukushima Daiichi Nuclear Power Plant

A. Toyoshima, K. Takamiya[1], and H. Furutani[2]

Institute for Radiation Sciences, Osaka University
[1]Institute for Integrated Radiation and Nuclear Science, Kyoto University
[2]Center for Scientific Instrument Renovation and Manufacturing Support, Osaka University

INTRODUCTION: First preliminary removal of the fuel debris remaining in the Units 1, 2, and 3 of Fukushima Daiichi Nuclear Power Plant is planned to be started soon. In the removal, fine particles containing alpha emitters of actinides such as ^{235}U and ^{239}Pu are concerned to be yielded in cutting the debris to put into a sealed container. We, therefore, aim to develop a novel real-time detection method for the dispersed particles using Aerosol Time-Of-Flight Mass Spectrometer (ATOFMS). At present, an improved type of ATOFMS is newly developed and an enlargement and condensation apparatus to increase the detection sensitivity of ATOFMS by enlarging its non-detectable tiny particles to detectable-sized ones before the ATOFMS measurement. In the present study, we performed SEM-EDS measurements for the enlarged ^{238}U particles using the apparatus.

EXPERIMENTS: Primary particles were produced from a $(U_{0.5}Zr_{0.5})O_2$ pellet by laser ablation in a closed chamber. The produced particles were swept out of the chamber by carrier gas of dried air and were continuously collected in water using PILS (Particle Into Liquid Sampler, Metrohm AG). Then, the water containing the primary particles were sprayed using a supersonic atomizer and sprayed droplets were dried by dried air at a flow rate of 0.1 L/min in a chamber. The droplets were also dried by passing a diffusion dryer filled with silica gel. The resulting dried particles were collected on a carbon tape attached in a small impactor. After transporting collected particle samples to KURNS, SEM-EDS measurement of the samples was carried out. Energy of bombarded electrons was 15 kV. SEM images and X-ray spectra of the samples were taken for lots of enlarged particles found on the carbon tapes.

RESULTS: In Fig. 1, a SEM image of the collected particles is shown. Many of the enlarged particles are observed. These have a diameter of around 1 μm, which is suitable to the particle detection using ATOFMS. Element composition was also obtained by the EDS analysis. Results showed U, Zr, O, Si, Fe, etc. were contained in the particles. This means that primary $(U_{0.5},Zr_{0.5})O_2$ particles were successfully enlarged, although other elements probably originated from the apparatus used are also contained in the particles.

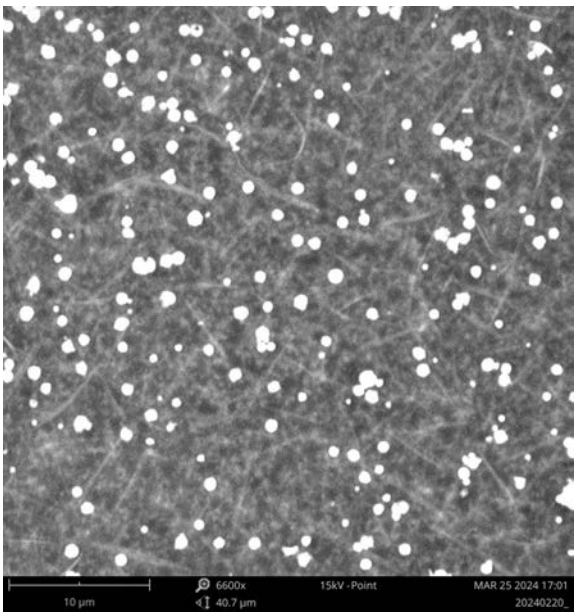

Fig. 1. SEM image of enlarged particles collected on a carbon tape.

CO12-4

Radiation degradation in ^{3}He-filled position sensitive neutron detector

H. Ohshita[1], H. Endo[1], T. Seya[1], S. Matoba[1] and M. Hino[2]

[1]*Institute of Materials Structure Science, KEK*
[2]*Institute for Integrated Radiation and Nuclear Science, Kyoto University*

INTRODUCTION: At the Materials and Life Science Experimental Facility (MLF) of J-PARC, over 5000 ^{3}He gas-filled position sensitive neutron detectors (^{3}He-PSNDs) have been installed to conduct neutron experiments. ^{3}He-PSNDs are cylindrical gas-proportional counters filled with a mixture of ^{3}He and CF_4 gases. ^{3}He gas serves as a neutron converter for detecting neutrons, and the charged particles emitted by the ^{3}He(n,p)^{3}H reaction are detected as neutron hits. CF_4 gas exhibits a high stopping power against charged particles, as well as a high electron drift velocity, and affords stable operation in large intense radiation environments owing to its enhanced rate characteristics. Recently, ^{3}He-PSNDs used in MLF have shown remarkable radiation degradation, and a decrease in the pulse height has been reported. This has been attributed to the accumulation of F_2 gas generated as a dissociation product of CF_4 gas. During the gas amplification process, chemically active neutral radicals, such as $\dot{F}$ (superscript letters indicate that they are neutral radicals), are produced. These neutral radicals react with the anode wire near the electron avalanche, rapidly producing metal fluorides. Concurrently, $\dot{F}$ accumulation in the form of F_2 occurs in the chamber gas, causing the gas amplification to decrease owing to electron attachment. Partially, recombination, which entails neutral radical consumption, occurs and leads to the regeneration of CF_4. Given the likely dependence of the amount of $\dot{F}$ produced on the magnitude of the gas amplification and the existence of further $\dot{F}$ consumption processes, the changes in the pulse height are expected to eventually stabilize. Based on this premise, we performed a neutron irradiation test on the ^{3}He-PSND at KUR CN-3.

EXPERIMENTAL RESULTS: The experimental setup was constructed downstream of the movable slit in KUR CN-3. The ^{3}He-PSND was covered by a shield made of B_4C resin with an aperture size of 1 cm × 4 cm. The ^{3}He-PSND has an outer diameter of 1/2 in and an active length of 150 mm. The filling pressures of ^{3}He and CF_4 were 6 atm and 0.56 atm, respectively. The width of the movable slit was set to 5 mm, and the neutron beam was irradiated for approximately 16 h. The beam power of KUR is 1 MW, and the expected neutron intensity is 7.6×10^5 neutrons/s·cm^2. The slit was periodically closed to measure the pulse-height distribution. The applied voltages were 1.8 kV and 1.3 kV for heavy irradiation with a 5 mm slit width and for measuring the pulse-height distribution, respectively. During heavy irradiation, the pulse-height distribution could not be measured owing to pile-up; therefore, the current of the high-voltage module was measured. Figure 1 shows the trend of ^{3}He-PSND currents during the neutron irradiation tests. A gradual decrease in the current and eventual saturation were observed immediately after the start of the experiment. The pulse-height distribution was measured in locations where the respective data were missing. Figure 2 shows a comparison of the pulse-height distributions immediately after and at the end of the experiment. At the end of the experiment, the distribution showed evident deformation, indicating the impact of radiation degradation. In the future, we plan to conduct another neutron irradiation test in the MLF to elucidate the radiation degradation mechanism and to select alternative gases.

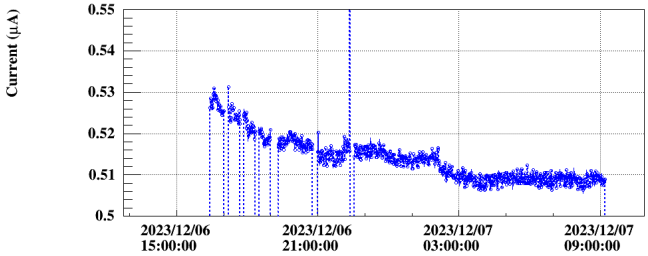

Figure 1. Trend of 3He-PSND currents during the neutron irradiation tests.

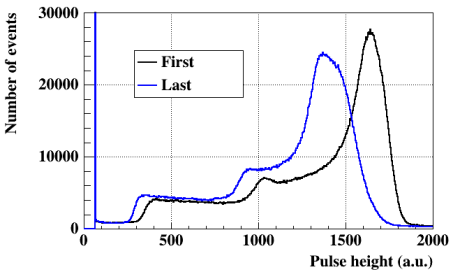

Figure 2. Comparison of pulse-height distributions.

CO12-5

Neutron Refectometry under High Shear in Narrow Gap for Tribology Study

T. Hirayama, N. Yamashita and M. Hino[1]

Department of Mechanical Engineering and Science, Graduate School of Engineering, Kyoto University
[1]Institute for Integrated Radiation and Nuclear Science, Kyoto University

INTRODUCTION: Many studies of mechanical sliding surfaces under lubricated conditions have been carried out in the field of tribology. The trend towards using low viscosity oil to reduce frictional losses has made lubricant additives particularly important in protecting surfaces. It is therefore essential to evaluate the properties of the adsorbed layer formed in a narrow gap by additives under lubricated conditions. In this study, neutron reflectometry was used to investigate the structure of adsorbed additive layers under high shear rates simulating liquid lubricated conditions. Neutron reflectometry is widely used in the field of tribology, but it is mainly used to evaluate the thickness and density of adsorbed additive layers in a static state. In contrast, few *operando* analyses have been carried out in a shear field and the change in the structure of the adsorbed layer formed by an additive on the sliding surfaces has not been clarified.

EXPERIMENTS: The purpose of this study was to establish an *operando* analysis method for evaluating the interfacial structure of an adsorbed layer formed by an additive on a metal surface under fluid lubrication conditions in which a non-contact condition was maintained with a few micrometers gap. To achieve this, we developed an analytical method that combines the use of a neutron reflectometer SOFIA (BL16, MLF) with that of a previously developed parallel-disk viscometer with a narrow gap kept by an aerostatic bearing system. The Si block with thin Cu layer sputtered on by KUR-IBS was used as a sample surface in the study.

RESULTS: Prior to the experiment, 40 μL of d-Sq containing PMA was added to the gap. First, the reflectivity profile was obtained without rotation to evaluate the structure of the polymer adsorbed layer formed on the surface of the Cu layer in the static condition. Then the upper sample was rotated and the reflectivity profile was obtained again. The rotation speed was 100 rpm, so the shear rate was 6.1×10^4 s^{-1}. The footprint was 2×10 mm and the reflectivity profile was obtained with an incident angle of only 0.6º. The reflectivity profiles obtained are shown in Fig. 1(a). This graph shows the results in air (top) and with lubricant under static (middle) and shear (bottom) conditions with fitting lines and offsets in the vertical axis direction for better visibility. The SLD profiles obtained from the fitting analysis are shown in Fig. 1(b). The surface structure of the Cu layer was first determined by fitting the reflectivity profile measured in air without lubricant. Then the structural changes in the adsorbed PMA layer without and with rotation of the top sample were evaluated using a model in which the state of the Cu layer determined by the measurement in air was assumed to remain unchanged and the adsorbed PMA layer was assumed to form on top of the Cu layer. The results show that both the thickness and density of the adsorbed PMA layer became lower under high shear than under static conditions, indicating that the polymer additive desorbed from the Cu surface, probably due to the high shear force. This finding will be useful in the design of lubricant additives that can function under a wide range of lubrication and high shear rate conditions.

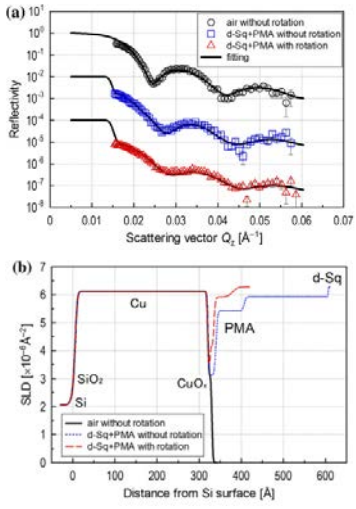

Fig. 1. Reflectivity profiles and estimated SLD profiles.

CO12-6

A trial to analyze the texture of the excavated medieval *Haji*-ware of different colour by INAA

M. Tomii, K. Takamiya[1], M. Inagaki[1], Y. Chiba[2], A. Ito[2], M. Kidachi[3], and H. Yoshii[2]

Faculty of Literature, Taisho University
[1]Institute for Integrated Radiation and Nuclear Science, Kyoto University
[2] Graduate School of Letters, Kyoto University
[3] College of Letters, Ritsumeikan University

INTRODUCTION: A collection of low-temperature-fired pottery (*Haji*-ware) of 14th century archaeologically excavated from a shallow deposition in the campus of Kyoto University [1]is analyzed. It is composed of the classic four types of the medieval Kyoto: white larger bowl, white tiny cup, reddish medium-sized plate, and reddish small plate. In Kyoto as the old capital, *Haji*-ware has long been used for ceremony/ritual even after introduction of higher-temperature-fired ceramics. Its marked difference in colour –white/red– has been widely recognized among archaeologists, and they also have known that such difference in colour corresponds with that in the manner to produce the shape of its base and rim. However, the reason for the colour difference remains to be explained; whether it resulted from the different group of potters, the different manner of making by the same potter group, or whatever. This study therefore tries to check in detail by using INAA whether the colour difference resulted from the different texture of pottery or not.

EXPERIMENTS: Conventional INAA was applied to determine the elemental composition of samples of the *Haji*-ware, each of whose main body had been drilled, or scraped, by the alumina drill into fine powder as a sample after removing off the very surface, and then had been enclosed in a polyethylene bag [2]. Every of above-mentioned four types of the *Haji*-ware has seven samples respectively from different pieces. Each of the 28 samples was neutron-irradiated at Pn-3 (1 MW for 90 seconds) for short-lived nuclides, and at Pn-2 (5 MW for 1 hours) for long-lived ones. The comparative standards were irradiated with the same condition. The gamma-ray spectrometry of the irradiated samples was performed after the irradiation. Along with the comparison method, the k_0-standardization method was also performed. For the latter method, three standard elements were prepared as a comparator: Au, Lu and Zr.

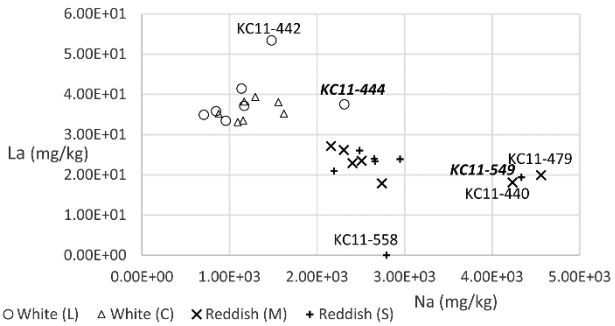

Fig 1 Distribution of 28 samples on the concentrations combination of Na with La.

RESULTS: By the k_0-standardization method, concentrations of two elements (K and Na) in every 28 sample were determined with irradiation by Pn-3, and La and Eu were also determined in most samples, though Mg, Ti, V, Mn, Ga and Sm were in around fifteen samples. The determination by comparison method for samples irradiated by Pn-3 and Pn-2, as well as the k_0-standardization method on ones by Pn-2, were not completed so far. However, it can be pointed out from the k_0-standardization method on short-lived nuclides that Na and La show clear difference in concentration to divide 28 samples into two groups, which correspond with the colour groups except for one sample: KC11-444 (Fig.1). As for the separately distributed samples, KC11-442, 440 and 479 represented slightly different colour in appearance, though KC11-549 did not. The result might suggest that the colour difference was brought by the texture difference, though KC11-444 might indicate another reason for the colour difference: the firing technique for instance.

REFERENCES:

[1] M. Tomii *et al.*, Annu. Rept. of Archaeological Researches in KU sites for 2013. (2015) 5-122.
[2] J. Sterba, J. Radio. Nucl. Chem., **316** (2018) 753-759

Neutron scattering imaging with Talbot-Lau interferometer at CN-3

Y. Seki, Y. Terakawa, M. Li[1], M. Hino[2]

Institute of Multidisciplinary Research for Advanced Materials, Tohoku University
[1]Department of Nuclear Engineering, Kyoto University
[2]Institute for Integrated Radiation and Nuclear Science, Kyoto University

INTRODUCTION: A neutron phase imaging system with a Talbot-Lau interferometer is installed at CN-3 port in the Kyoto University reactor [1]. The Talbot-Lau interferometer, a type of grating interferometer, can produce differential-phase and scattering images [2], in addition to conventional absorption images. For application research, scattering imaging is particularly attractive since it is sensitive to small-angle scattering intensity and can investigate microstructures in samples. The spatial scale that the visibility imaging can explore is characterized by an autocorrelation length ξ. This scale is related to the interferometer parameters as $\xi = \lambda z_s/d_2$, where λ is the neutron wavelength, d_2 is the period of an analyzer grating, and z_s is the distance between the sample and the analyzer grating. The autocorrelation length is usually changed by adjusting the sample position. The contrast of visibility imaging is described as $V_0/V_s(\xi) = \exp[-\Sigma(1 - G(\xi))]$, where V_0 is the visibility of interference fringes without samples, V_s is with samples, Σ is a macroscopic cross section of small-angle scattering which is proportional to λ^2, and G is an autocorrelation function of microstructures. Due to these wavelength dependences, the autocorrelation length is not obvious in the case of measurement with white beams. Therefore, we calibrate the autocorrelation lengths in visibility imaging with the current setup at CN-3 by measuring a sample whose visibility signal at a certain autocorrelation length is well known through the wavelength-resolved method.

EXPERIMENTS: The sample consisted of monodisperse silica spheres with a nominal diameter of 0.2 μm, randomly packed in a quartz cell. Visibility images of this sample have been observed using the time-of-flight method at BL22 RADEN in J-PARC MLF. At the CN-3, visibility imaging was performed through phase-stepping method with eight steps at seven sample positions. The exposure time was 3200 s per phase step at a reactor thermal power of 1 MW.

RESULTS: Figure 1 illustrates an example of visibility image of the sample. The visibility values were averaged within the sample region and plotted in Fig. 2. The effective wavelength that reproduced the results the RADEN was 2.95 Å, which was 9.3% larger than the design wavelength of the interferometer. The autocorrelation lengths were also evaluated using this effective wavelength with a pitch of 9.0 μm for the analyzer grating.

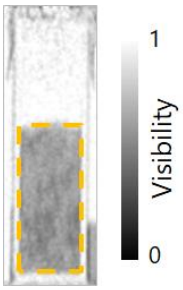

Fig. 1. Visibility image of the monodisperse silica spheres.

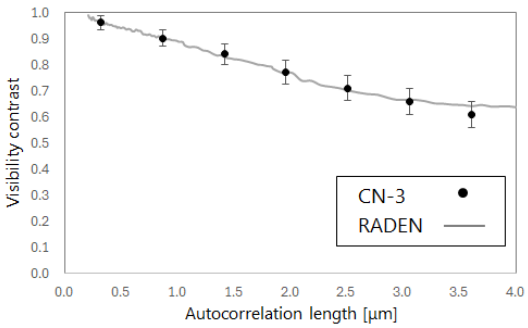

Fig. 2. Average visibility values versus calibrated autocorrelation lengths.

REFERENCES:

[1] Y. Seki *et al.*, Nucl. Instr. and Meth., **186** (1981)115-120.
[2] M. Strobl, Scientific Reports, **4** (2014) 7243.

A New Technique of the Micro bunch Interval Measurement in an Electron Linear Accelerator

T. Takahashi

Institute for Integrated Radiation and Nuclear Science, Kyoto University

INTRODUCTION: The coherent radiation from short bunches of electrons in an accelerator is useful of analysis of the specification of bunches. For example, it has been used in the high-resolution diagnosis of electron distribution in a bunch [1]. There are two kinds of detector in the millimeter wave region. One is a diode detector with narrow band and high-speed response. The other is a liquid-helium cooled bolometer with wide band and slow response. A bolometer is usually used with a spectrometer, for example a monochromator or an interferometer. In the experiment of FY2023 the time-domain measurement with a diode detector was used for the analysis of the micro bunch interval.

EXPERIMENTS: The experiment was performed with KURNS-LINAC. The energy of the electron beam was 39 MeV and the peak beam current measured by CT was 1.6 A. The repetition rate of the macro pulse was 60 pulses/s. Coherent transition radiation from a titanium window was guided to the coherent radiation beam line [2] in the experimental room and detected by a diode detector. This detector was a zero-biased W-band amplitude detector SFD-753114-103-10SF-N1 (SAGE Millimeter, Inc.), which detection speed was 10 ns. The output signal of the detector was measured by the mixed domain oscilloscope MDO3104 (Tektronix, inc.) with the bandwidth of 1 GHz and the sampling rate of 5 GS.

RESULTS: The observed waveform of coherent transition radiation in the case of 47-ns macro pulse is shown in Fig. 1. The number of micro bunches is 61 and the micro bunch interval is 770 ps calculated from the frequency of RF of 1.3 GHz. Fig. 2 shows the waveform in the case of 2-ns macro pulse. In both figures the sampling interval is 0.2 ns because of the sampling rate of the oscilloscope. The rise time of the signal is also slow. It is experimentally revealed that it is difficult to measure the micro bunch interval by a diode detector.

REFERENCES:

[1] Y. Shibata *et al.,* Phys. Rev. E, **50** (1994) 1479-1484.
[2] T. Takahashi *et al.,* Rev. Sci. Instrum., **69** (1998) 3770.

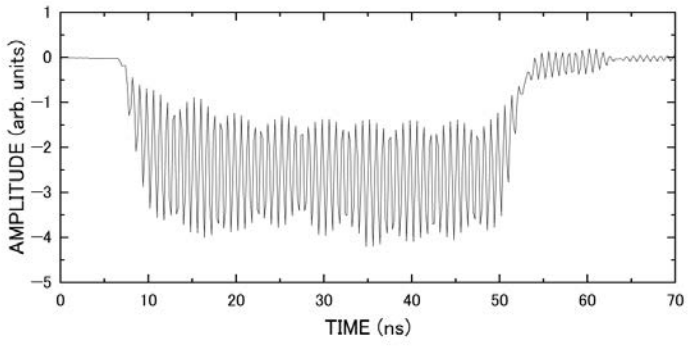

Fig. 1. The observed waveform of coherent transition radiation for 47-ns pulsed beam.

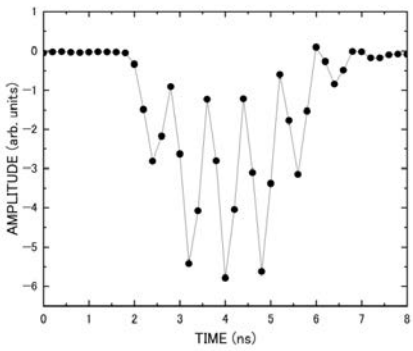

Fig. 2. The observed waveform of coherent transition radiation for 2-ns pulsed beam.

CO12-9

Study of Isotope Separation via Chemical Exchange Reaction

R. Hazama, P. Kumsut, T. Yoshimoto, A. Rittirong[1], C. Pitakchaianan, K. Kosinarkaranun, Y. Sakuma[2], T. Fujii[3], T. Fukutani[4], Y. Shibahara[4], and T. Kishimoto[1]

Graduate School of Human Environment, Osaka Sangyo University
[1]Research Center for Nuclear Physics, Osaka University
[2]Laboratory for Advanced Nuclear Energy, Tokyo Institute of Technology
[3]Graduate School of Engineering, Osaka University
[4]Institute for Integrated Radiation and Nuclear Science, Kyoto University

INTRODUCTION: Chemical isotope separation for calcium and lithium has been studied by liquid-liquid extraction (LLE) with DC18C6 crown-ether [1]. This report describes separation coefficient (ε) under the various temperature (1/T), ranging from -15℃ to 45℃, for the two phase (aqueous and organic) reaction of LLE.

EXPERIMENTS: Chemical Isotopic exchange occurs according to the following chemical exchange reaction: $^{6}Li^{+}_{(aq)} + {}^{7}LiL^{+}_{(org)} \rightarrow {}^{6}Li^{+}_{(aq)} + {}^{7}LiL^{+}_{(org)}$ (1)
, where L represents macrocyclic polyether (DC18-crown-6).

RESULTS: As shown in Fig. 1, the separation coefficient (ε) has the following temperature dependence with the second order polynomial, based on the Bigeleisen's new theory [2].

$$\varepsilon = \frac{a}{T^2} + \frac{b}{T} \quad , \quad \ln \alpha = a\left(\frac{\triangle M}{MM'}\right) + b\,\delta(r^2) + \ln K_{hf} \qquad (2)$$

, where a, and b are the scaling factor of nuclear mass effect and nuclear field effect, respectively. (T: Temperature(Kelvin), M and M': mass of heavier and lighter isotope, respectively, and △M is the difference of isotopes, and $\delta\langle r^2\rangle$ and $\ln K_{hf}$ are the change in mean square of the charge radii and the contribution of hyperfine splitting based on the nuclear spin, respectively.)

1/T (K)	℃	$\delta\langle r^2\rangle$ (fm^2)	ΔM/MM'	α(org)±σ	ε(α(org)−1)
0.003876	−15	−0.731	0.0238	0.990±0.005	0.010
0.003663	0			0.994±0.004	0.006
0.00339	22			0.991±0.003	0.009
0.003145	45			0.994±0.005	0.006

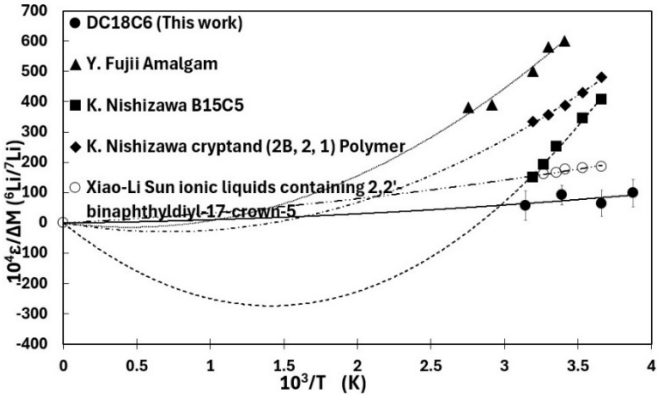

Fig. 1. Separation coefficient (ε) of litium based on the various extraction temperature ranging from –15℃ to 45℃, compared with the past research on amalgam, B15C5, cryptand, and ionic liquids [3,4,5,6].

The contribution ratio of nuclear field and nuclear spin to the nuclear mass effect are obtained as −0.039 and -1.6×10^{-7}, respectively (a and b are 4.6×10^{2} and 0.58, respectively.)

REFERENCES:

[1] A. Rittirong, Doctor Thesis, OSU (2022).
[2] J. Bigeleisen, J.Am.Chem.Soc., 118 (1996) 3676 .
R. Hazama *et al.,* arXiv0710.3840.
[3] Y. Fujii *et al.,* J. Nucl. Sci.Tec., 39 (2002) 413.
[4] K. Nishizawa *et al.,* J. Nucl. Sci. Tec., 21 (1984) 694.
[5] K. Nishizawa *et al.,* J. Nucl. Sci. Tec., 21 (1984) 133.
[6] X.Sun *et al.,* J. Nucl. Sci. Tec., 52 (2015) 332.

CO12-10

Development of Radiation Monitor for Space weather measuring Electrons (RMS-e) for the Himawari-10 satellite

K. Sakaguchi[1] and T. Namekawa[1]

[1]*National Institute of Information and Communications Technology*

INTRODUCTION: Monitoring of the radiation environment in geostationary orbit around the Earth are very important for space weather forecast. However, the instruments on board the currently operating Himawari 8 and 9 meteorological satellites have an insufficient energy range to fully monitor the space radiation environment. Therefore, we are developing Radiation Monitor for Space weather measuring Electrons (RMS-e) instrument installed on the next Himawari meteorological satellite. The RMS-e instrument is designed to measure the energy and flux of electrons between 50 keV and 6 MeV, which is an energy range sufficient to monitor the space radiation environment, using layered solid-state detectors (SSDs) made of silicon semiconductors. We conducted an evaluation of the measurement range for electron energy and energy resolution of > 2 MeV electrons by irradiating electrons emitted by Kyoto University, Institute for Integrated Radiation and Nuclear Science - Linear Accelerator (KURNS-LINAC) to the engineering model (EM) of RMS-e.

EXPERIMENTS: RMS-e EM was installed in the irradiation room and the monoenergetic electron beam generated by LINAC was injected perpendicular to the layered SSDs. The electron energies injected into RMS-e EM were 2.2, 2.6, 2.95, 3.3, 3.9, 4.5, 5.25, 6, and 7 MeV. The outer circumference of RMS-e EM was covered with lead blocks for radiation protection. Commands to control RMS-e EM were entered remotely from a PC installed in the control room.

RESULTS: Figure 1 shows the energy spectrum obtained using RMS-e EM for all incident electron beams (2.2, 2.6, 2.95, 3.3, 3.9, 4.5, 5.25, 6, and 7 MeV). For electron beams with energies below 6 MeV, a clear spectral peak is obtained. The shift of the peaks to lower energies and the tail of the peak extending to the low energy side are due to scattering of electrons by the Al shield to block low energy electrons. The energy resolution based on the full width half maximum of the peaks is about 10% for electrons below 5 MeV. The energy resolution for the 2.2 MeV electron beam can be affected by background γ-rays with energies of 1-1.5 MeV. The energy resolution also tends to be poor due to the small number of electrons detected, as RMS-e must be evaluated at very low beam flux. The result of this evaluation indicates that RMS-e can measure electrons between 2.2 MeV and 5 MeV with an energy resolution better than 10%, which is sufficient performance to measure the radiation environment in geostationary orbit around the Earth.

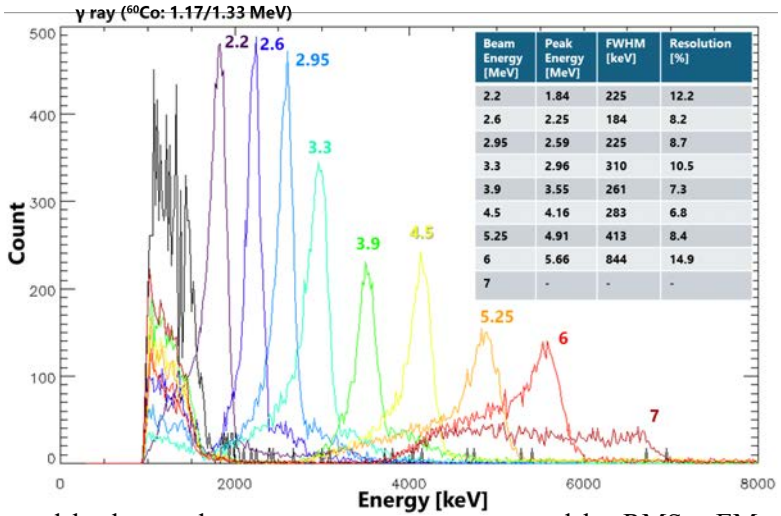

Figure 1. The electron and background γ-ray energy spectra measured by RMS-e EM under the irradiation of monoenergetic electron beams (2.2, 2.6, 2.95, 3.3, 3.9, 4.5, 5.25, 6 and 7 MeV). The total number of electrons / γ-rays is the same for each energy spectrum.